

## Crystal Structure and Magnetic Properties of $\text{FeTe}_2\text{O}_5\text{X}$ ( $\text{X} = \text{Cl}, \text{Br}$ ): A Frustrated Spin Cluster Compound with a New Te(IV) Coordination Polyhedron

Richard Becker,<sup>†</sup> Mats Johansson,<sup>\*†</sup> Reinhard K. Kremer,<sup>‡</sup>  
Hans-Henning Klaus,<sup>§</sup> and Peter Lemmens<sup>§</sup>

Contribution from the Department of Inorganic Chemistry, Stockholm University, S-106 91 Stockholm, Sweden, the Max-Planck Institute for Solid State Research, Heisenbergstrasse 1, D-70569 Stuttgart, Germany, and the Institute for Physics of Condensed Matter, TU Braunschweig, D-38106 Braunschweig, Germany

Received July 4, 2006; E-mail: matsj@inorg.su.se

**Abstract:** A new layered transition metal oxohalide,  $\text{FeTe}_2\text{O}_5\text{Cl}_x\text{Br}_{1-x}$ , has been identified. It crystallizes in the monoclinic space group  $P2_1/c$ . The unit cell for  $\text{FeTe}_2\text{O}_5\text{Br}$  is  $a = 13.3964(8)$ ,  $b = 6.5966(4)$ ,  $c = 14.2897(6)$  Å,  $\beta = 108.118(6)^\circ$ , and  $Z = 8$ . The layers are built of edge sharing  $[\text{FeO}_6]$  octahedra forming  $[\text{Fe}_4\text{O}_{16}]^{20-}$  units that are linked by  $[\text{Te}_4\text{O}_{10}\text{X}_2]^{6-}$  groups. The layers have no net charge and are only weakly connected via van der Waals forces to adjacent layers. There are four crystallographically different Te atoms, and one of them displays a unique  $[\text{TeO}_2\text{X}]$  coordination polyhedron ( $\text{X} = \text{Cl}, \text{Br}$ ). Magnetic susceptibility measurements show a broad maximum typical for 4-spin clusters of coupled Fe(III) ions in the high-spin state. Evidence for magnetic instabilities exists at low temperatures, which have been confirmed with specific heat experiments. A theoretical modeling of the susceptibility concludes a frustration of the intra-tetramer anti-ferromagnetic exchange interaction.

### Introduction

Magnetic frustration results from a competition of different interactions, and the atomic spins in a 'frustrated' magnet cannot simultaneously minimize the energies of their local interactions.<sup>1</sup> A strongly frustrated system is said to have a high density of low-energy excitations or "soft modes" that correspond to fluctuations between these energetically equivalent configurations. Frustration can be most easily studied in geometrically frustrated magnets having competing interactions among the atomic spins. Most geometrically frustrated physical systems are identified based on topological considerations from structural data bases, and surprisingly few synthesis concepts have been developed to systematically design novel systems. However, during the past few years a synthesis concept for finding new low-dimensional spin frustrated inorganic compounds has been developed. This work is the outcome of attempts to find new compounds that comprise  $\text{Fe}^{3+}$  ions.

The synthesis concept is based on forming oxohalides involving p-element cations that are in the oxidation state where they have a stereochemically active lone pair (e.g.,  $\text{Te}^{4+}$ ,  $\text{Se}^{4+}$ ,  $\text{As}^{3+}$ , and  $\text{Sb}^{3+}$ ). The presence of a stereochemically active lone pair will allow for asymmetric or one-sided coordination around the lone pair cation. In addition also such a strong Lewis acid (e.g.,  $\text{Te}^{4+}$ ) preferably only forms bonds to oxygen while the

transition metal cations bond to both oxygen and halides in an oxohalide environment. As a result, both the stereochemically active lone pair and the halide ions will function as terminating species opening up the structures and increase the possibilities for low dimensional arrangements. This synthesis concept has previously successfully been applied with the aim to search for new compounds with reduced dimensionality in the arrangement of late transition metal cations, and several such compounds have been found; for example,  $\text{Cu}_2\text{Te}_2\text{O}_5\text{X}_2$  ( $\text{X} = \text{Cl}, \text{Br}$ ),<sup>2</sup>  $\text{CuSb}_2\text{O}_3\text{Br}$ ,<sup>3</sup>  $\text{Ni}_5(\text{TeO}_3)_4\text{Cl}_2$ ,<sup>4</sup> and  $\text{Cu}_4\text{Te}_5\text{O}_{12}\text{Cl}_4$ .<sup>5</sup>

The objective of this work was to search for new low-dimensional compounds in the Fe(III)–Te(IV)–O–X ( $\text{X} = \text{Cl}, \text{Br}$ ) systems. The work resulted in the new synthetic compounds  $\text{FeTe}_2\text{O}_5\text{Cl}$  and  $\text{FeTe}_2\text{O}_5\text{Br}$  as well as the compound  $\text{FeTe}_2\text{O}_5\text{Cl}_{0.5}\text{Br}_{0.5}$ . To the best of our knowledge, the only previously described iron halide tellurite is the mineral rodalquilarite  $\text{Fe}_2\text{H}_3(\text{TeO}_3)_4\text{Cl}$ .<sup>6,7</sup> In addition, the cluster compounds  $(\text{Fe}(\text{CO}_3)_2\text{Cl}(\text{TeCl}_2)_2(\text{Te}_2\text{Cl}_{10}))$  and  $(\text{Fe}(\text{CO}_3)_2(\text{Te}_4)(\text{TeCl}_2))$  have been suggested to contain some  $\text{Te}^{4+}$ .<sup>8</sup>

- (2) Johansson, M.; Törnroos, K. W.; Mila, F.; Millet P. *Chem. Mater.* **2000**, *12*, 2853–2857.
- (3) Mayerova, Z.; Johansson, M.; Lidin, S. *J. Solid State Chem.* **2005**, *178*, 3471–3475.
- (4) Johansson, M.; Törnroos, K. W.; Lemmens, P.; Millet P. *Chem. Mater.* **2003**, *15*, 68–73.
- (5) Takagi, R.; Johansson, M.; Gnezdilov, V.; Kremer, R. K.; Brenig, W.; Lemmens, P. *Phys. Rev. B* **2006**, *74*, 014413/1–8.
- (6) Dusaouy, Y.; Protas, J. *Acta Crystallogr.* **1969**, *B25*, 1551–1558.
- (7) Feger, C. R.; Kolis, J. W.; Gorny, K.; Pennington, C. *J. Solid State Chem.* **1999**, *143*, 254–259.
- (8) Eveland, J. R.; Whitmire, K. H. *Angew. Chem.* **1996**, *108*, 741–743.

<sup>†</sup> Stockholm University.

<sup>‡</sup> Max-Planck Institute for Solid State Research.

<sup>§</sup> Institute for Physics of Condensed Matter.

(1) Greedan, J. E. *J. Mater. Chem.* **2001**, *11*, 37–53.

## Experimental Section

The synthesis of  $\text{FeTe}_2\text{O}_5\text{Cl}$ ,  $\text{FeTe}_2\text{O}_5\text{Br}$ , and  $\text{FeTe}_2\text{O}_5(\text{Cl}_{0.5}\text{Br}_{0.5})$  were made by chemical reactions in sealed evacuated silica tubes. The preparation of  $\text{FeTe}_2\text{O}_5\text{Cl}$  and  $\text{FeTe}_2\text{O}_5\text{Br}$  were made from  $\text{TeO}_2\text{:Fe}_2\text{O}_3\text{:FeX}_3$  ( $\text{X} = \text{Cl}, \text{Br}$ ) mixed in the stoichiometric molar ratios 6:1:1 in a mortar and placed in silica tubes (length  $\sim 5$  cm), which were then evacuated and sealed off. The tubes were subsequently heated in a muffle furnace at 510 °C for 48 h for  $\text{FeTe}_2\text{O}_5\text{Cl}$  and at 480 °C for 70 h for  $\text{FeTe}_2\text{O}_5\text{Br}$ , respectively. The preparation of the mixed Cl/Br compound was made in the same manner from a mixture of  $\text{TeO}_2\text{:TeBr}_4\text{:Fe}_2\text{O}_3\text{:FeCl}_3$  in the stoichiometric molar ratio 45:3:10:4 that was heat-treated in a muffle furnace at 530 °C for 46 h.

The synthesis products of all preparations were a mixture of  $\text{FeTe}_2\text{O}_5\text{X}$  crystals and a yellow/brown powder of undetermined composition. The  $\text{FeTe}_2\text{O}_5\text{Cl}$  crystals were bright yellow, and the  $\text{FeTe}_2\text{O}_5\text{Br}$  crystals were more dark yellow, almost orange. The color of the mixed Cl/Br compound was in-between the two end components.

The chemical composition of the synthesis products were characterized in a scanning electron microscope (SEM, JEOL 820) with an energy-dispersive spectrometer (EDS, LINK AN10000).

Single-crystal X-ray data were collected on an Oxford Diffraction Xcalibur3 diffractometer with use of graphite-monochromatized  $\text{Mo K}\alpha$  radiation,  $\lambda = 0.71073$  Å, for all three synthesized compounds. The intensities of the reflections were integrated using the software supplied by the manufacturer. Numerical absorption correction was performed with the programs X-red<sup>9</sup> and X-Shape.<sup>10</sup> The structures were solved by direct methods using the program SHELXS97<sup>11</sup> and refined by full-matrix least-squares on  $F^2$  using the program SHELXL97.<sup>12</sup> All atoms are refined with anisotropic temperature parameters. Crystal data for  $\text{FeTe}_2\text{O}_5\text{Cl}$  and  $\text{FeTe}_2\text{O}_5\text{Br}$  are reported in Table 1.

The multi-crystal sample used for magnetic susceptibility and specific heat measurements was manually selected based on crystal color and shape and characterized by use of powder X-ray diffraction (PXRD) data obtained with a Guiner-Hägg focusing camera with subtraction geometry.  $\text{Cu K}\alpha_1$  radiation ( $\lambda = 1.54060$  Å) was used, and silicon,  $a = 5.43088(4)$  Å, was added as an internal standard. The recorded films were read in an automatic film scanner, and the data were evaluated using the programs SCANPI<sup>13</sup> and PIRUM.<sup>14</sup> The sample used for magnetic susceptibility measurements was found to be phase pure from powder X-ray data. The Cl-phase was found to have the unit cell parameters  $a = 13.187(5)$ ,  $b = 6.589(2)$ ,  $c = 14.155(3)$  Å, and  $\beta = 108.77(2)^\circ$ , which are in good agreement with the single-crystal diffraction data.

The magnetic susceptibilities of  $\text{FeTe}_2\text{O}_5\text{Cl}$  and  $\text{FeTe}_2\text{O}_5\text{Br}$  were measured with a MPMS SQUID magnetometer (Quantum Design) between 2 and 350 K in magnetic fields up to 5 T. The samples (typically  $m \approx 35$  mg) were loosely filled into Gelatine capsules, the magnetization of which was measured separately and subtracted from the total magnetization. The heat capacity of  $\text{FeTe}_2\text{O}_5\text{Cl}$  was measured with a PPMS system (Quantum Design) between 2 and 200 K on a polycrystalline piece ( $\approx 11$  mg) in vanishing external magnetic field. The  $^{57}\text{Fe}$  Mössbauer spectroscopy experiment was performed on the same sample ( $\text{X} = \text{Cl}$ ) at 295 K in transmission geometry using a  $^{57}\text{Co}$ -in-Rh source.

## Results and Discussion

**Crystal Structure.** The solid solution  $\text{FeTe}_2\text{O}_5\text{Cl}_x\text{Br}_{1-x}$  crystallizes in the monoclinic system, space group  $P2_1/c$ . Single-

**Table 1.** Crystal Data for  $\text{FeTe}_2\text{O}_5\text{Cl}$  and  $\text{FeTe}_2\text{O}_5\text{Br}$

emp form	$\text{FeTe}_2\text{O}_5\text{Cl}$	$\text{FeTe}_2\text{O}_5\text{Br}$
fw	426.50	470.96
temp	291(2) K	291(2) K
wavelength	0.71073	0.71073
cryst syst	monoclinic	monoclinic
space group	$P2_1/c$	$P2_1/c$
unit cell dimensions	$a = 13.1526(9)$ Å $b = 6.5950(4)$ Å $c = 14.1454(9)$ Å $\beta = 108.771(6)^\circ$	$a = 13.3964(8)$ Å $b = 6.5966(4)$ Å $c = 14.2897(9)$ Å $\beta = 108.118(6)^\circ$
vol (Å <sup>3</sup> )	1161.73(13)	1200.18(13)
Z	8	8
density (calcd)	4.877 g cm <sup>-3</sup>	5.213 g cm <sup>-3</sup>
abs coeff	12.843 mm <sup>-1</sup>	18.646 mm <sup>-1</sup>
abs correction	numerical	numerical
$F(000)$	1496	1640
cryst color	bright yellow	dark yellow
cryst habit	thin flake	thin flake
cryst size (mm)	0.09*0.05*0.007	0.12*0.08*0.008
$\theta$ range for data collection	4.01–27.44°	3.97–30.93°
index ranges	$-17 \leq h \leq 17$ $-8 \leq k \leq 8$ $-18 \leq l \leq 18$	$-19 \leq h \leq 19$ $-9 \leq k \leq 9$ $-20 \leq l \leq 20$
reflns collected	17234	22687
independent reflns	2577 [R(int) = 0.0825]	3820 [R(int) = 0.0617]
completeness to $\theta$	96%	99%
= max range		
refinement method	full-matrix least-squares on $F^2$	full-matrix least-squares on $F^2$
data/restraints/parameters	2577/0/163	3820/0/163
goodness-of-fit on $F^2$	1.076	0.924
final R indices [ $I > 2\sigma(I)$ ]	$R_1 = 0.0410$ $wR_2 = 0.0979$	$R_1 = 0.0317$ $wR_2 = 0.0582$
R indices (all data)	$R_1 = 0.0596$ $wR_2 = 0.1046$	$R_1 = 0.0533$ $wR_2 = 0.0617$
largest diff. peak and hole	2.229 and $-2.044$	3.047 and $-1.570$

crystal experimental parameters for  $\text{FeTe}_2\text{O}_5\text{Cl}$  and  $\text{FeTe}_2\text{O}_5\text{Br}$  are listed in Table 1. In addition to the end compositions, also a crystal with  $x = 0.5$  has been investigated and found to have the unit cell parameters  $a = 13.2722(8)$  Å,  $b = 6.5965(4)$  Å,  $c = 14.2351(9)$  Å, and  $\beta = 108.021(1)^\circ$ . The structural details for the compound within the solid solution are not further discussed below, but structure data are deposited at the Fachinformationzentrum Karlsruhe (Abt. PROKA, 76344 Eggenstein-Leopoldshafen, Germany; fax: +49-7247-808-666; e-mail: crysdata@fiz-karlsruhe.de; request deposit numbers CSD-416642, CSD-416643, and CSD-416644). EDS analysis on several crystals from all three compounds confirms the stoichiometry of the heavier elements including the 50/50 ratio of chlorine and bromine in the mixed compound. The structure description below is based on  $\text{FeTe}_2\text{O}_5\text{Br}$ ; however, the Cl and the Cl/Br analogues are very similar.

The crystal structure is layered, and only weak van der Waals interactions connect the layers so that each layer can be considered as an infinite two-dimensional molecule (see Figure 1). The halide anions and the stereochemically active lone pairs of the  $\text{Te}^{4+}$  cations, designated E, protrude from the layers. Bond valence sum calculations discussed below have been performed according to Brown and Altermatt,<sup>15</sup> and the operational definition of a bond according to Brown (4% of the cation valence) is used to determine the primary bonding distance for the ions.<sup>16</sup> The  $R_0$  values used for these calculations are  $R_0(\text{Te}-$

(9) X-RED, Version 1.22; STOE & Cie GmbH: Darmstadt, Germany, 2001.  
 (10) X-SHAPE revision 1.06; STOE & Cie GmbH: Darmstadt, Germany, 1999.  
 (11) Sheldrick, G. M. SHELXS-97—Program for the Solution of Crystal Structures; Göttingen, 1997.  
 (12) Sheldrick, G. M. SHELXL-97—Program for the Refinement of Crystal Structures; Göttingen, 1997.  
 (13) Johansson, K. E.; Palm, T.; Werner, P. E. J. Phys. Sci. Instrum. **1980**, *13*, 1289–1291.  
 (14) Werner, P. E. Arkiv Kemi **1969**, *31*, 513–516.

(15) Brown, I. D.; Altermatt, D. Acta Crystallogr. **1985**, *B41*, 244–247.  
 (16) Brown, I. D. The Chemical Bond in Inorganic Chemistry: The Bond Valence Model; Oxford University Press: New York, 2002.

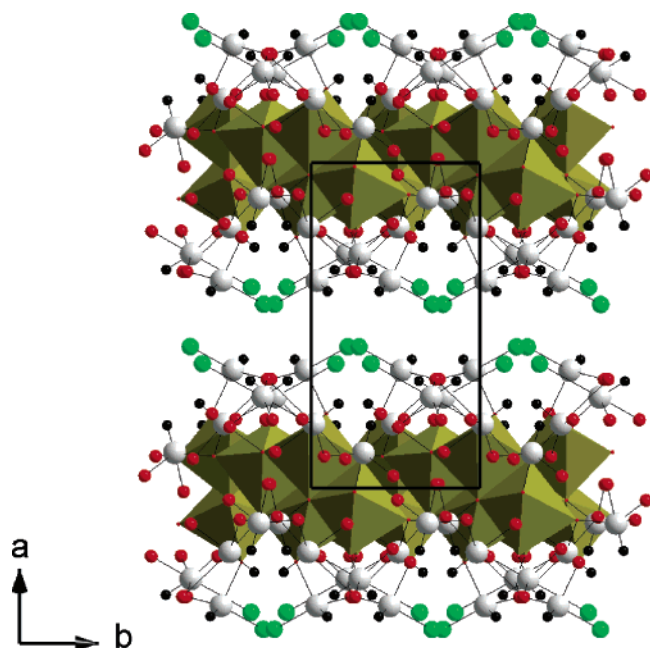


**Figure 1.** Crystal structure of  $\text{FeTe}_2\text{O}_5\text{X}$  is layered with only weak van der Waals interactions in between the layers. The halide ions and the stereochemically active lone pair, E, can be observed protruding from the layers.  $\text{Te}^{4+}$  is gray,  $\text{O}^{2-}$  is red,  $\text{Cl}^-/\text{Br}^-$  are green, the  $[\text{FeO}_6]$  octahedra are brown, and E is represented by a black sphere.

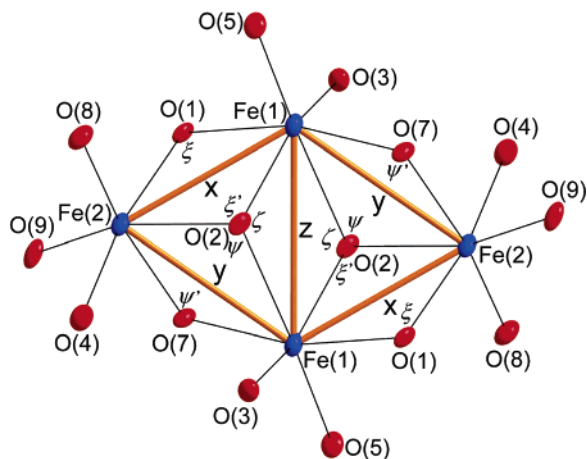


**Figure 2.** Single  $[\text{Fe}_4\text{O}_{16}]^{20-}$  building block consisting of four edge sharing  $[\text{FeO}_6]$  octahedra. See Table 2 for a list of intra Fe–Fe distances and Fe–O–Fe angles.

$R_0(\text{Te–Br}) = 2.55$ ,<sup>17</sup>  $R_0(\text{Te–Cl}) = 2.37$ ,<sup>18</sup> and  $R_0(\text{Fe–O}) = 1.765$ .<sup>19</sup>

There are two crystallographically different  $\text{Fe}^{3+}$  positions. Both of them have a distorted  $[\text{FeO}_6]$  octahedral coordination. Four such octahedra are connected via edge sharing to form a  $[\text{Fe}_4\text{O}_{16}]^{20-}$  unit where the four  $\text{Fe}^{3+}$  ions are in the same plane and form a rhomboid (see Figure 2).

There are four crystallographically different  $\text{Te}^{4+}$  cations, which all can be described as having an asymmetric one-sided coordination with different number of ligands.  $\text{Te}(1)$  is one-sided coordinated to three oxygens at distances around 1.89 Å, giving it a tetrahedral  $[\text{Te}(1)\text{O}_3\text{E}]$  coordination. Two additional

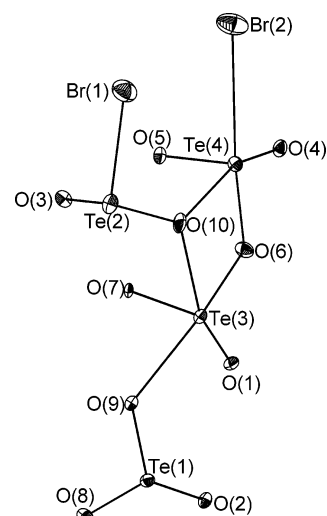


**Figure 3.** Planar  $[\text{Te}_4\text{O}_{10}\text{X}_2]^{6-}$  group showing the various coordination polyhedra around the  $\text{Te}^{4+}$  cations.

oxygen anions can be observed at 2.805(7) and 2.963(8) Å, which is clearly outside the primary bonding distance of 2.66 Å for Te–O bonds. The  $\text{Te}(2)$  cation coordinates two oxygens and one halide giving it a unique  $[\text{Te}(2)\text{O}_2\text{BrE}]$  coordination. To the best of our knowledge, the present compounds are the first where  $\text{Te}^{4+}$  has the classical one-sided three-coordination with both oxygen and a halide instead of only one of the two ligands. There are also two additional halide anions present at longer distances from  $\text{Te}(2)$ . For the Br phase these are positioned 3.212(1) and 3.333(7) Å away from the  $\text{Te}^{4+}$  cation; for the Cl phase they are positioned 3.168(7) and 3.183(3) Å away. The Brown definition of a bond yields a limit of 3.05 Å for Te–Cl bonds and 3.22 Å for Te–Br bonds, so the long-distanced halides in the present compounds are just at the border of what can be considered as belonging to the primary coordination sphere and are not regarded as bonded.  $\text{Te}(3)$  coordinate three oxygen anions at approximately 1.92 Å and two additional ones at 2.477(4) and 2.549(4) Å, which results in a one-sided  $[\text{Te}(3)\text{O}_{3+2}\text{E}]$  coordination resembling a greatly distorted octahedron.  $\text{Te}(4)$  has also three short Te–O distances of approximately 1.90 Å as well as two additional ligands, an oxygen anion at 2.549(4) Å and a bromine anion at 3.1146(8) Å, resulting in a distorted  $[\text{Te}(4)\text{O}_{3+1}\text{BrE}]$  octahedral coordination. The additional ligands for  $\text{Te}(3)$  and  $\text{Te}(4)$  are positioned inside the primary coordination sphere for the Te–ligand bonds according to Brown. The four different Te polyhedra are connected via corner and edge sharing to form a  $[\text{Te}_4\text{O}_{10}\text{X}_2]^{6-}$  group (see Figure 3).

The Bond valence sum calculations gives values close to the expected valences for all ions except for one of the halide ions (see Supporting Information). The bromide in the  $[\text{TeO}_2\text{BrE}]$  tetrahedron has a bond valence sum of 1.08 vu and is thus close to the expected value. However, the bromide in the  $[\text{TeO}_{3+1}\text{BrE}]$  octahedron gets a value of only 0.22 vu (0.19 vu for the chloride in  $\text{FeTe}_2\text{O}_5\text{Cl}$ ), indicating that it more takes the role of a counterion than being integrated in the covalent/ionic network. This situation is common in oxohalides and has been reported in, for example,  $\text{Sb}_8\text{O}_{11}\text{X}_2$  ( $\text{X} = \text{Cl}, \text{Br}$ )<sup>20</sup> and  $\text{Ca}_2\text{CuTe}_4\text{O}_{10}\text{Cl}_2$ .<sup>21</sup>

(17) Brown, I. D. Bond valence sum parameters. [http://www.ccp14.ac.uk/ccp/web-mirrors/i\\_d\\_brown/bond\\_valence\\_param/](http://www.ccp14.ac.uk/ccp/web-mirrors/i_d_brown/bond_valence_param/).

(18) Brese, N. E.; O’Keeffe, M. *Acta Crystallogr.* **1991**, *B47*, 192–197.

(19) Liu, W.; Thorp, H. H., *Inorg. Chem.* **1993**, *32*, 4102–4105.

(20) Mayerová, Z.; Johnsson, M.; Lidin S. *Solid State Sci.* **2006**, *8*, 849–854.

(21) Takagi, R.; Johnsson, M. *Acta Crystallogr.* **2005**, *C61*, i106–i108.



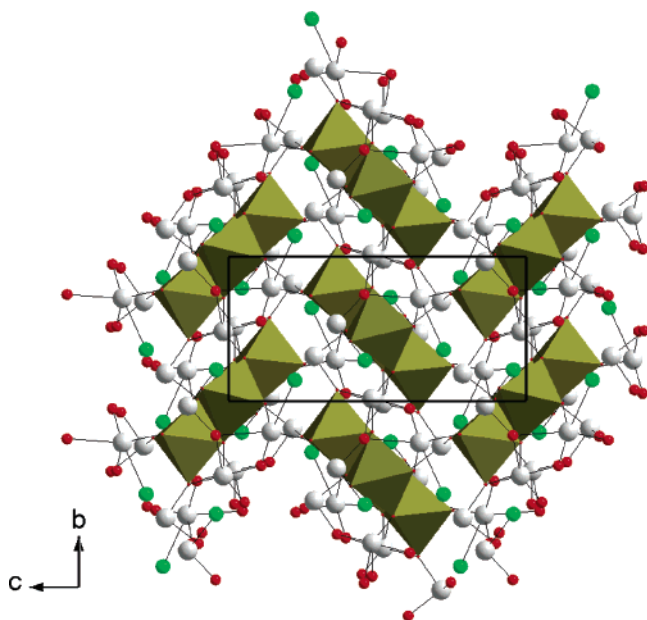


**Figure 4.** Single layer of  $\text{FeTe}_2\text{O}_5\text{X}$ . The  $[\text{Fe}_4\text{O}_{16}]^{20-}$  groups are held together to form the layers by common oxygen ions with the  $[\text{Te}_4\text{O}_{10}\text{X}_2]^{6-}$  groups. The color codes are the same as in Figure 1.

Each layer in the crystal structure is made up of the two different building blocks; the  $[\text{Fe}_4\text{O}_{16}]^{20-}$  groups and the  $[\text{Te}_4\text{O}_{10}\text{X}_2]^{6-}$  groups. The  $[\text{Te}_4\text{O}_{10}\text{X}_2]^{6-}$  groups can be seen forming sublayers sandwiching the  $[\text{Fe}_4\text{O}_{16}]^{20-}$  groups (see Figure 1). There are no bonds formed in between two different  $[\text{Te}_4\text{O}_{10}\text{X}_2]^{6-}$  groups nor between two different  $[\text{Fe}_4\text{O}_{16}]^{20-}$  groups, but instead the  $[\text{Te}_4\text{O}_{10}\text{X}_2]^{6-}$  groups are connected to the  $[\text{Fe}_4\text{O}_{16}]^{20-}$  groups via common oxygens to build up the layers, thereby reaching charge neutrality between the two negatively charged groups (see Figure 4). The layers extend along the  $bc$ -plane and they are completely separated from adjacent layers so that only weak van der Waals interactions connect the layers. The shortest Fe–Fe distance in between two  $[\text{Fe}_4\text{O}_{16}]^{20-}$  groups within the same layer is  $\sim 4.76$  Å, and the shortest Fe–Fe distance in between two layers is  $\sim 10.1$  Å. This large separation and the lack of direct bonds in between the layers suggest that there are very weak magnetic interactions in between two layers.

**Magnetic Characterization and Specific Heat.** The magnetic susceptibility of  $\text{FeTe}_2\text{O}_5\text{X}$  ( $X = \text{Cl}, \text{Br}$ ) is characterized by a Curie–Weiss behavior for temperatures above about 100 K and a broad maximum at  $T_{\text{max}} = 41.8$  K (48.4 K) in  $\text{FeTe}_2\text{O}_5\text{Cl}$  ( $\text{FeTe}_2\text{O}_5\text{Br}$ ). This resembles low-dimensional or frustrated anti-ferromagnets.<sup>2,22,23</sup> Field-cooled and zero-field-cooled measurements show no traceable hysteresis. The reciprocal susceptibilities can be well-fitted to a modified Curie–Weiss law (see Figure 5a inset):

$$\chi_{\text{mol}} = C/(T - \theta_{\text{CW}}) + \chi_{\text{dia}} \quad (1)$$

The Curie constant  $C$  is related to the effective magnetic  $\mu_{\text{eff}}$  moment according to

$$C [\text{cm}^3/\text{mol}] = (\mu_{\text{eff}} [\mu_{\text{B}}])^2 \times 0.125051 \quad (2)$$

$\chi_{\text{dia}}$  is a temperature-independent contribution that relates to the

(22) Lemmens, P.; Güntherodt, G.; Gros, C. *Phys. Rep.* **2003**, *375*, 1–103.

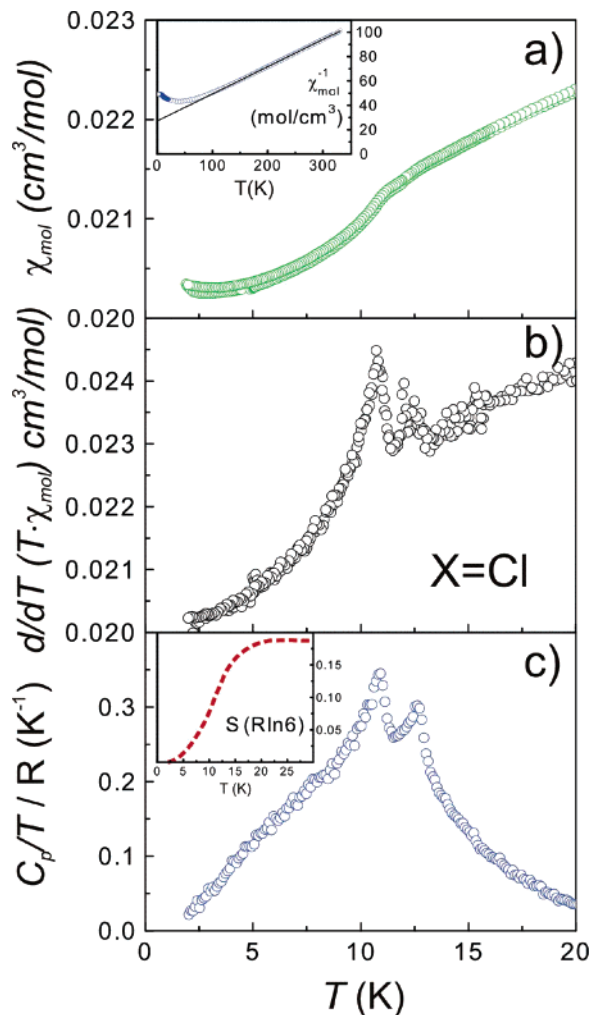


**Figure 5.** (a) Magnetic susceptibility of  $\text{FeTe}_2\text{O}_5\text{Cl}$  measured at 0.1 T. The inset shows the reciprocal susceptibility. The solid line represents a fit to a modified Curie–Weiss law (eq 1) with an effective magnetic moment of  $6.04 \mu_{\text{B}}$  and a paramagnetic Curie temperature of  $-124(2)$  K. (b) Temperature derivative  $d/dT (\chi_{\text{mol}} \cdot T)$ . (c) Specific heat capacity. The inset gives the entropy derived from the specific heat after subtracting an estimated phonon contribution.

diamagnetic susceptibilities of the closed core shells. Using Pascal’s increments, we estimate  $\chi_{\text{dia}}$  to be  $-124 \times 10^{-6} \text{ cm}^3/\text{mol}$  and  $-134 \times 10^{-6} \text{ cm}^3/\text{mol}$  for  $\text{FeTe}_2\text{O}_5\text{Cl}$  and  $\text{FeTe}_2\text{O}_5\text{Br}$ , respectively.<sup>24</sup> The paramagnetic Curie temperature  $\theta_{\text{CW}}$  is negative for both compounds, indicating predominant anti-ferromagnetic exchange interactions.  $\theta_{\text{CW}}$  amounts to  $-124(2)$  K and to  $-98(2)$  K for  $X = \text{Cl}$  and  $\text{Br}$ , respectively. The effective magnetic moments obtained from the fits are very close to  $5.92 \mu_{\text{B}}$  as expected for  $\text{Fe}^{3+}$  with a  $d^5$  electronic configuration and a high-spin  ${}^6S$  ( $S = 5/2$ ,  $g = 2$ ) ground state. For  $X = \text{Cl}$ ,  $\mu_{\text{eff}}$  is fitted to  $6.04(2) \mu_{\text{B}}$ ; for  $X = \text{Br}$ ,  $\mu_{\text{eff}}$  amounts to  $5.6(1) \mu_{\text{B}}$ . To account for these differences we consider a small error in the determination of the sample mass or some paramagnetic inclusions in the tested crystals.

At  $\sim 10$  K the susceptibility of  $\text{FeTe}_2\text{O}_5\text{Cl}$  shows a kink (Figure 5a), apparently due to the onset of long-range afm ordering. The derivative  $d/dT (\chi_{\text{mol}} \cdot T)$  and the specific heat

(23) Gros, C.; Lemmens, P.; Vojta, M.; Valenti, R.; Choi, K.-Y.; Kageyama, H.; Hiroi, Z.; Mushnikov, N.V.; Goto, T.; Johansson, M.; Millet, P. *Phys. Rev.* **2003**, *B67*, 174405/1–5.

(24) Selwood, P. W. *Magnetochemistry*, 2nd ed.; Interscience: New York, 1956.

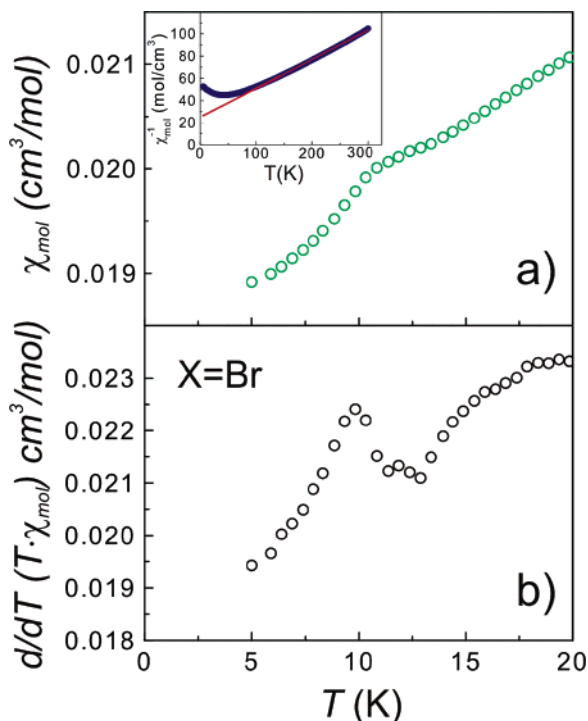


**Figure 6.** (a) Magnetic susceptibility of  $\text{FeTe}_2\text{O}_5\text{Br}$  measured at 5 T. The inset shows the reciprocal susceptibility. The solid line represents a fit to a modified Curie–Weiss law (eq 1) with an effective magnetic moment of  $5.6 \mu_B$  and a paramagnetic Curie temperature of  $-98(2)$  K. (b) Displays the temperature derivative  $d/dT (\chi_{\text{mol}} \cdot T)$ .

capacity reveal two  $\lambda$ -type anomalies in this temperature range indicating that long-range ordering occurs in a two-step transition split by about 2 K (Figure 5b,c). For  $\text{FeTe}_2\text{O}_5\text{Br}$  a similar kink anomaly is observed at 9.7 K, however with only one anomaly resolved (Figure 6a,b).

Results of the Mössbauer experiments on  $\text{X} = \text{Cl}$  at room temperature are shown in the lower inset of Figure 7. The observed doublet is characteristic for a Fe site experiencing an electric field gradient. The asymmetry in the absorption strength between both lines and in the shape of the individual lines is due to the two crystallographically different Fe sites in the crystal. The spectrum has been evaluated using the Mössbauer fitting program RECOIL<sup>25</sup> in the thin absorber approximation using two Lorentzian doublets with equal intensities. Both doublets show nearly identical isomeric shifts of  $\text{IS}_1 = 0.19(2)$  mm/s and  $\text{IS}_2 = 0.18(6)$  mm/s with respect to an iron foil absorber at room temperature. The evaluated quadrupole splittings are  $\text{QS}_1 = 0.69(4)$  mm/s and  $\text{QS}_2 = 0.6(1)$  mm/s. These values are typical for high spin Fe(III).<sup>26</sup> The occupation of all five 3d orbitals by a single electron leads in total to a spherical charge distribution with no contribution to the electric field gradient. Therefore, the evaluated electric field gradients are due to the neighboring ionic charges in the two different low-symmetry lattice positions of the Fe ions. The evaluated line widths (HWHM) are  $\Gamma_1 = 0.11(2)$  mm/s and  $\Gamma_2 = 0.20(7)$  mm/s. The line width of doublet 2 is slightly enhanced with respect to the natural line width  $\Gamma = 0.097$  mm/s. This may be associated with a distribution of the local electric field gradient or the limited signal-to-noise ratio on this small sample.

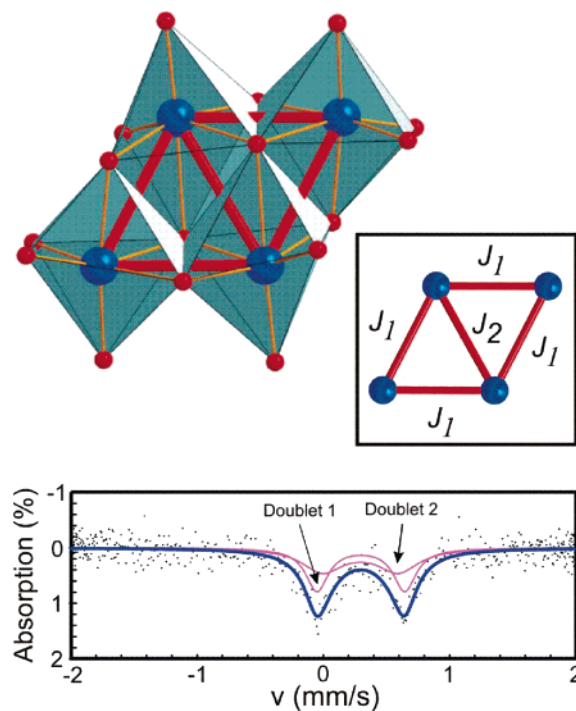


**Figure 7.** Sketch of a  $\text{Fe}^{3+}$  tetramer in the crystal structures of  $\text{FeTe}_2\text{O}_5\text{X}$  ( $\text{X} = \text{Cl}, \text{Br}$ ). The thick solid red lines indicate the shortest Fe–Fe distances (right inset). The lower inset gives the result of a Mössbauer experiment on  $\text{X} = \text{Cl}$  at room temperature with fits consisting of two doublets (thin solid lines) and the sum (thick solid line) as described in the text.

**Table 2.** Fe–Fe Distances and Fe–O–Fe Angles within a  $[\text{Fe}_4\text{O}_{16}]^{20-}$  Group

	$\text{FeTe}_2\text{O}_5\text{Cl}$	$\text{FeTe}_2\text{O}_5\text{Br}$
X	3.152(2) Å	3.159(1) Å
Y	3.328(2) Å	3.343(1) Å
Z	3.427(3) Å	3.435(2) Å
$\xi_1$	101.4(3)°	101.7(2)°
$\xi_2$	99.0(3)°	99.5(2)°
$\psi$	95.5(2)°	95.9(1)°
$\psi'$	110.0(3)°	110.2(2)°
$\psi''$	101.9(3)°	101.7(2)°

To model the magnetic susceptibilities of  $\text{FeTe}_2\text{O}_5\text{X}$  ( $\text{X} = \text{Cl}, \text{Br}$ ), we apply a cluster approach. Guided by the crystal structure we assume that the exchange coupling between the magnetic moments within the  $\text{Fe}^{3+}$  tetramer exceeds the coupling in-between them. We also describe the exchange coupling by a Heisenberg-type Hamiltonian and thus neglect, in a first approximation, anisotropic terms (e.g., due to zero-field splitting (typically 0.5 K) that emerge from an admixture of excited states by spin–orbit coupling). This approach seems justified in view of the essentially spin-only moments of the  $3d^5$  electronic configuration that is confirmed by the high-temperature susceptibility data.

In an Fe tetramer (Figure 7) the distorted octahedra are connected via common edges and the superexchange paths connecting neighboring  $\text{Fe}^{3+}$  ions involve the two  $\text{O}^{2-}$  ions in the shared edge with bonding angles  $\sim 95$ – $110^\circ$  (see Table 2). Four  $\text{Fe}^{3+}$  ions form a rhomboid with exchange couplings along the edges and one across two opposite  $\text{Fe}^{3+}$  ions. If we assume that the exchange couplings along the edges are identical and given by  $J_1$  and the exchange parameter across the diagonal is given by  $J_2$ , we arrive at the following Hamiltonian:

(25) Lagarec, K. *Recoil Version 1.02*; University of Ottawa: Ottawa, 1998.

(26) May, L. *An Introduction to Mössbauer Spectroscopy*; Adam Hilger: London, 1971.

$$H = -2J_1(\vec{S}_1\vec{S}_3 + \vec{S}_2\vec{S}_3 + \vec{S}_2\vec{S}_4 + \vec{S}_1\vec{S}_4) - 2J_2\vec{S}_1\vec{S}_2 \quad (3)$$

for which the energy levels are given by<sup>27</sup>

$$E_{\text{tet}} = -J_1\{S^{\text{T}}(S^{\text{T}} + 1) - S^{\text{I}}(S^{\text{I}} + 1) - S^{\text{II}}(S^{\text{II}} + 1)\} - J_2\{S^{\text{I}}(S^{\text{I}} + 1) - S_1(S_1 + 1) - S_2(S_2 + 1)\} \quad (4)$$

wherein  $S^{\text{T}}$ ,  $S^{\text{I}}$ , and  $S^{\text{II}}$  are the quantum numbers to the spin operators:

$$\vec{S}^{\text{T}} = \sum_{i=1}^4 \vec{S}_i \quad (5a)$$

$$\vec{S}^{\text{I}} = \vec{S}_1 + \vec{S}_2, \quad \vec{S}^{\text{II}} = \vec{S}_3 + \vec{S}_4 \quad (5b)$$

For high-spin  $\text{Fe}^{3+}$   $S_i = 5/2$  and  $S^{\text{I}}$  and  $S^{\text{II}}$  can take the spin values 0, 1, ..., 5. Using the Van Vleck approximation,<sup>28</sup> the effective magnetic moment  $\mu_{\text{eff}}$  is given by

$$\mu_{\text{eff}}^2(T) = g^2 \frac{\sum_{S^{\text{T}}} S^{\text{T}}(S^{\text{T}} + 1)(2S^{\text{T}} + 1) \exp\left(-\frac{E_{\text{tet}}(S^{\text{T}})}{k_{\text{B}}T}\right)}{\sum_{S^{\text{T}}} (2S^{\text{T}} + 1) \exp\left(-\frac{E_{\text{tet}}(S^{\text{T}})}{k_{\text{B}}T}\right)} \quad (6)$$

For the susceptibility of a tetramer one obtains

$$\chi_{\text{mol}}^{\text{tet}}(T) = \mu_0 \frac{N_{\text{A}} \mu_{\text{B}}^2 \mu_{\text{eff}}^2(T)}{3k_{\text{B}}T} \quad (7)$$

To consider the exchange coupling between the Fe tetramers, we apply a mean-field approach and calculate the susceptibility  $\chi_{\text{mol}}^{\text{MF}}$  according to

$$\chi_{\text{mol}}^{\text{MF}} = \frac{\chi_{\text{mol}}^{\text{tet}}}{1 - \chi_{\text{mol}}^{\text{tet}} \frac{2z'J'}{N_{\text{A}}g^2\mu_{\text{B}}^2}} + \chi_{\text{dia}} \quad (8)$$

where  $z'J'$  represents a mean exchange coupling of a Fe tetramer units to  $z'$  neighboring tetramer clusters and  $N_{\text{A}}$  is the Avogadro constant.

Fitting eq 8 to the measured molar susceptibilities ( $T > 15$  K) allows extracting the exchange parameters. The fits are displayed in Figure 8. The fits for  $\text{FeTe}_2\text{O}_5\text{Cl}$  and  $\text{FeTe}_2\text{O}_5\text{Br}$  result in antiferromagnetic exchange couplings  $J_1$  and  $J_2$  within a tetramer cluster. As a consequence of the same sign and magnitude of  $J_1$  and  $J_2$  as well as a triangular arrangement of the Fe atoms, the spin arrangement in the tetramer unit is essentially magnetically frustrated. The exchange coupling between the units is ferromagnetic. With  $z' \approx 6$ , the inter-cluster exchange constant  $J'$  is about a factor of 3–5 smaller than the intra-cluster exchange constant. Obviously, magnetic frustration and the reduced inter-cluster exchange are the reason for the small long-range ordering temperature  $T_{\text{N}}$ , viz. by the large frustration parameter  $f = |\theta_{\text{CW}}/T_{\text{N}}|$ .<sup>1</sup> Another reason for pro-

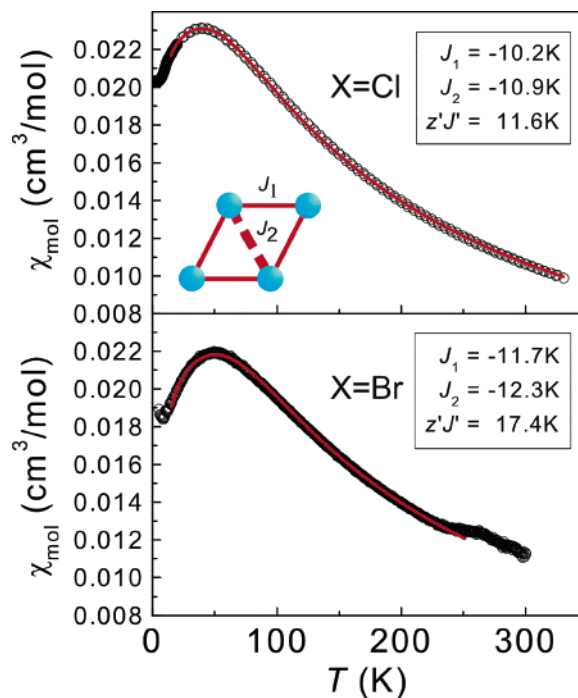


**Figure 8.** Molar magnetic susceptibilities of  $\text{FeTe}_2\text{O}_5\text{Cl}$  and  $\text{FeTe}_2\text{O}_5\text{Br}$ . The red solid line represents the calculated susceptibility according to eq 8 using the exchange constants given in the insets.

**Table 3.** Magnetic Parameters Determined from an Analysis of the Susceptibility and Specific Heat Measurements and the Frustration Parameter  $f = |\theta_{\text{CW}}/T_{\text{N}}|$  as Described in the Text

magnetic parameter	$\text{FeTe}_2\text{O}_5\text{Cl}$	$\text{FeTe}_2\text{O}_5\text{Br}$
$\theta_{\text{CW}}$ (K)	-124(2)	-98(2)
$\mu_{\text{eff}}/\mu_{\text{B}}$	6.04	5.6
$T_{\text{max}}$ (K)	41.8	48.4
$T_{\text{N}}$ (K)	11 / 12.6	9.7
$f =  \theta_{\text{CW}}/T_{\text{N}} $	11 / 10	10
$J_1$ (K)	-10.2	-11.7
$J_2$ (K)	-10.9	-12.3
$z'J'$ (K)	11.6	17.4

nounced fluctuations are the coincidence of weak anisotropy of the  $3d^5$  high spin configuration with the layered nature of the compound. The fluctuations are also evident from the small magnetic entropy at the transition temperature. Subtracting an estimated lattice contribution from the specific heat the entropy approximates to about 20% of  $R \ln(6)$  for  $X = \text{Cl}$ . This reduction is remarkable keeping in mind that quantum fluctuations are not involved. All derived magnetic parameters are summarized in Table 3.

The discussed magneto-structural correlations of  $\text{FeTe}_2\text{O}_5\text{X}$  are also evident from a comparison of intra Fe–Fe distances and Fe–O–Fe angles for the  $[\text{Fe}_4\text{O}_{16}]^{20-}$  groups that are listed in Table 2 with the magnetic parameters. The shortest inter Fe–Fe distances between the groups, 4.73 Å for  $X = \text{Cl}$  and 4.76 Å for  $X = \text{Br}$ , are considerably larger than the intra group Fe–Fe distances. Therefore the spin cluster character of the material is preserved, meaning that long-range ordering is largely suppressed. The smaller transition temperature for  $X = \text{Br}$  should be based on a moderate weakening of the characteristic exchange paths that connect the  $[\text{Fe}_4\text{O}_{16}]^{20-}$  groups. The large variety of intra- and inter-group distances including competing interactions leads to the large variation of magnetic energy scales

(27) Flood, M. T.; Barraclough, C. G.; Gray, H. B. *Inorg. Chem.* **1969**, *8*, 1855–1859.

(28) Van Vleck, J. H. *The Theory of Electric and Magnetic Susceptibilities*; University Press: Oxford, 1932.

given by the Curie–Weiss temperature, the maximum position and the ordering effects.

### Conclusions

The new isostructural layered compounds  $\text{FeTe}_2\text{O}_5\text{X}$  ( $\text{X} = \text{Cl}, \text{Br}$ ) as well as the solid solution  $\text{FeTe}_2\text{O}_5\text{Cl}_{0.5}\text{Br}_{0.5}$  have been synthesized in sealed evacuated silica tubes. The compounds crystallize in the centrosymmetric space group  $P2_1/c$ , and each layer consists of groups of four edge sharing  $[\text{FeO}_6]$  octahedra that are connected into  $[\text{Fe}_4\text{O}_{16}]^{20-}$  groups. These groups are further connected via oxygen bonds to the  $\text{Te}^{4+}$  ions to build up the layers. The layers have no net charges, and only weak van der Waals interactions connect them.

The four  $\text{Fe}^{3+}$  ions in the  $[\text{Fe}_4\text{O}_{16}]^{20-}$  groups form a tetramer in the form of a rhomboid, and the exchange couplings are supposed to be along the edges ( $J_1$ ) and across two opposite  $\text{Fe}^{3+}$  ions ( $J_2$ ). The magnetic properties are described within a cluster approach of antiferromagnetically coupled tetramers including spin frustration and a ferromagnetic inter-tetramer interaction. From crystal chemistry point of view, the title compounds are unique in two ways: they are the first

compounds found in the systems  $\text{Fe}^{3+}\text{--Te}^{4+}\text{--O--X}$  ( $\text{X} = \text{Cl}, \text{Br}$ ) and, to the best of our knowledge, they are also the first compounds showing the unique  $[\text{TeO}_2\text{XE}]$  tetrahedron around  $\text{Te}^{4+}$ .

**Acknowledgment.** We thank Dr. M. Valldor for performing a part of the magnetic susceptibility measurements. This work has been carried out through financial support from the Swedish Research Council, the German Science Foundation (DFG), and the scientific program Highly Frustrated Magnetism supported by the European Science Foundation (ESF).

**Supporting Information Available:** Manufacturers of the chemicals used in the preparations of  $\text{FeTe}_2\text{O}_5\text{Cl}$ ,  $\text{FeTe}_2\text{O}_5\text{Br}$ , and  $\text{FeTe}_2\text{O}_5\text{Cl}_{0.5}\text{Br}_{0.5}$ ; atomic coordinates and bond distances for  $\text{FeTe}_2\text{O}_5\text{Cl}$  and  $\text{FeTe}_2\text{O}_5\text{Br}$ ; EDS analysis of the chemical composition in crystals of the three compounds; powder X-ray diffraction pattern for  $\text{FeTe}_2\text{O}_5\text{Cl}$ . This material is available free of charge via the Internet at <http://pubs.acs.org>.

JA064738D